

Orbital schwannomas: findings from magnetic resonance imaging in 62 cases

Y Wang and LH Xiao

Abstract

Purpose To evaluate the diagnostic value of magnetic resonance imaging (MRI) and illustrate the common MRI features of orbital schwannoma.

Methods We reviewed 62 consecutive cases of pathologically proven orbital schwannoma investigated by MRI. All cases were examined using T1- and T2-weighted images. Enhanced T1-weighted images were obtained after administration of gadopentetate dimeglumine. The images were analysed and compared.

Results Cone-shaped lesions were the most frequent (16, 26%), followed by dumbbell-shaped (10, 16%), oval (9, 15%) and round lesions (8, 13%). The most common site was the superior aspect of the orbit (17, 27%), followed by the medial superior (12, 19%) and the orbital apex (12, 19%). On unenhanced T1-weighted images, 53 (85%) lesions showed isointensity or small patches of hypointensity. The patterns of enhancement seen on T1-weighted images correlated with the signal characteristics of unenhanced T2-weighted images. Five patterns emerged in our series. Among these patterns, the most common sign, found in 18 (29%) cases, was peripheral (ring) enhancement on enhanced T1-weighted images, which showed peripheral isointensity with central hyperintensity on T2-weighted images. Lesions with homogeneous or heterogeneous enhancement were seen in 16 (26%) and 26 (42%) cases, respectively.

Conclusions MRI is a valuable diagnostic method for orbital schwannoma, particularly when contrast is applied. The locations and shapes of tumours can be seen distinctly. T1-weighted images are relatively nonspecific. T2-weighted and enhanced T1-weighted images provide information about the pathology of tumours. In particular, peripheral

enhancement should be considered a target sign of schwannoma.

Eye (2008) 22, 1034–1039; doi:10.1038/sj.eye.6702832; published online 20 April 2007

Keywords: neurilemmoma; orbital neoplasms; magnetic resonance imaging; diagnosis

Introduction

Schwannomas account for about 1–2% of all tumours in the orbit. They are well defined, encapsulated, slowly progressive tumours that originate in the peripheral nervous system. Early diagnosis and accurate evaluation of the extent of the schwannoma are essential for total removal of the tumour, preservation of normal anatomy, and restoration of visual acuity and ocular movements. Magnetic resonance imaging (MRI) is the method of choice for the examination of patients with suspected orbital schwannomas because of its high sensitivity, especially when contrast material is used. Published studies on MRI of orbital schwannomas are limited and systematic analyses are lacking. Most studies have been case reports^{1–4} or small series.^{5,6} Orbital schwannoma on MRI is usually described as a lesion that produces a low signal on T1-weighted images and a high signal on T2-weighted images, which can be homogeneously or heterogeneously enhanced. However, our data show that MRI of orbital schwannomas can yield more detailed information. We illustrate and analyse the common features of orbital schwannomas seen on MRI in 62 tumours.

Materials and methods

We reviewed 62 consecutive cases of pathologically proven orbital schwannoma

Institute of Orbital Diseases,
Armed Police General
Hospital, Beijing, China

Correspondence: LH Xiao,
69 Yongding Road, Haidian
District, Beijing 100039,
China
Tel: +86 10 8827 6687;
Fax: +86 10 6822 3307
E-mail: yieye@sina.com.

Received: 23 November
2006

Accepted in revised form:
16 March 2007

Published online: 20 April
2007

investigated by MRI at the Institute of Orbital Diseases, Beijing (China). Between September 1999 and June 2006, we examined 26 male and 36 female patients ranging in age from 11 to 70 years (average age 38 years). Scans were obtained with a 1.5-T superconductive MRI unit. T2-weighted axial and coronal images were obtained. T1-weighted axial, coronal, and oblique sagittal images were obtained before and after intravenous administration of gadopentetate dimeglumine (0.1 mmol/kg body weight). The enhanced scans were obtained immediately after injection in all cases. Slice thickness was 5 mm. The sizes and shapes of the tumours on MRI were recorded. The sites were classified as superior, medial superior, lateral, lateral inferior, lateral superior, medial, medial inferior or orbital apex.

Results

The shapes of the orbital schwannomas are summarised in Table 1. In 59 (95%) cases, the lesions had smooth margins; in the remaining three cases, which were recurrences, the lesions had ill-circumscribed margins.

The sites are listed in Table 2. In 10 (16%) cases, the lesion extended into the cranial cavity from the superior orbital fissure and in one (2%) case, it extended into the sphenomaxillary fossa from the inferior orbital fissure.

On unenhanced T1-weighted MRI, 33 (53%) of the lesions showed uniform isointensity relative to cerebral grey matter and 20 (32%) showed isointensity with small patches of hypointensity. Peripheral isointensity with central hypointensity was observed in eight (13%) lesions; the opposite phenomenon, peripheral hypointensity with central isointensity, was seen in only one case.

The signal intensity of the orbital schwannomas varied between T2- and enhanced T1-weighted images. Notably, the patterns of enhancement on T1-weighted images correlated with the signal characteristics of unenhanced T2-weighted images. Five patterns emerged in our study:

- (1) Homogeneous isointensity or hypointensity on T2-weighted images was seen in 16 (26%) of the

Table 2 Sites of tumors and frequency

Site of tumors in the orbit	Number of patients (%)
Superior	17 (27)
Medial superior	12 (19)
Orbital apex	12 (19)
Lateral	10 (16)
Lateral inferior	7 (11)
Medial inferior	3 (5)
Medial	1 (2)
Lateral superior	0 (0)

- tumours. Of these, 15 showed homogeneous enhancement on T1-weighted images (Figure 1) and one showed slightly inhomogeneous enhancement.
- (2) In 18 (29%) cases, peripheral (ring) enhancement was clearly seen on enhanced T1-weighted images. On T2-weighted images, these lesions showed peripheral isointensity with central hyperintensity (Figure 2). There were several patients with two or more enhancing rings in a lesion.
- (3) Two (3%) cases demonstrated peripheral (ring) non-enhancement with central enhancement on T1-weighted images after administration of contrast material. These two lesions showed peripheral hyperintensity with central isointensity on T2-weighted images (Figure 3).
- (4) In 17 (27%) lesions, the major portions were iso- to hypointense, with small patches of hyperintensity on T2-weighted images. Correspondingly, these lesions showed inhomogeneous enhancement, with small patches of hypointensity, following the injection of contrast material (Figure 4).
- (5) On T2-weighted images, the major portions of nine (15%) lesions were hyperintense, with small patches of iso- to hypointensity. On enhanced T1-weighted images, these lesions showed extensive non-enhancement with small patches of hyperintensity (Figure 5). Overall, the latter two types, representing heterogeneous enhancement, were seen in 26 (42%) cases.

Table 1 Shapes of tumors and frequency

Shape of tumors	Number of patients (%)
Cone-shaped	16 (26)
Dumbbell-shaped	10 (16)
Oval	9 (15)
Round	8 (13)
Polylobular	7 (11)
Fusiform	6 (10)
Irregular-shaped	5 (8)
Sausage-shaped	1 (2)

Discussion

Schwannomas are well-defined, encapsulated, slowly progressive benign tumours that develop as eccentric growths from the sheaths of peripheral nerves. They occur mainly in individuals aged between 20 and 50 years and have a predilection for the head and neck region. In the orbit, they account for 1–2% of all tumours. Since schwannomas occur infrequently, and have few typical signs, preoperative diagnosis is generally difficult. Correct diagnosis and accurate definition of the



Figure 1 (a) Axial T2-weighted image showing a mass with relatively homogenous hypointensity located behind the right globe to the orbital apex. (b) Axial gadolinium-enhanced T1-weighted image showing homogenous enhancement.

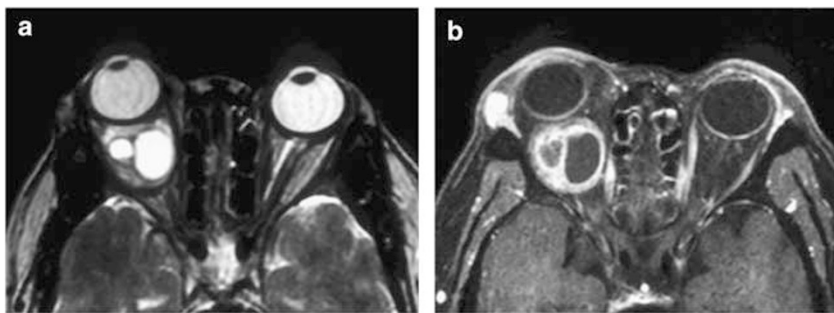


Figure 2 (a) Axial T2-weighted image showing an intraconal, round mass with peritumoural isointensity and central hyperintensity (two round areas). (b) Axial gadolinium-enhanced T1-weighted image showing two enhanced rings with central homogenous hypointensity.

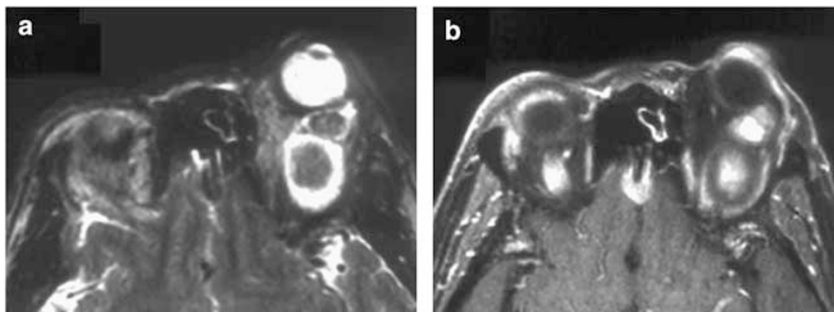


Figure 3 (a) Axial T2-weighted image showing a dumbbell-shaped mass with peritumoural hyperintensity and central isointensity located in the lateral orbit. (b) Axial gadolinium-enhanced T1-weighted image showing an enhanced centre with two peritumoural non-enhanced rings.

location and the extent of the lesion greatly facilitate successful surgical excision. However, published reports on MRI of orbital schwannomas are limited.¹⁻⁶ This study was undertaken to delineate the characteristics of orbital schwannomas on MRI and thereby help to increase the accuracy of preoperative diagnosis. We retrospectively analysed the MRI findings of 62 cases from the preceding 5 years. This number of cases is markedly higher than those in previous studies.

The orbit resembles a quadrilateral pyramid whose apex is formed by the optic canal and the superior orbital fissure. Accordingly, the shape of orbital schwannomas is usually oval or round. The tumours filling the orbital apex are cone-shaped. Those arising in the orbital apex and invading the cranial cavity from the superior orbital fissure are commonly dumbbell-shaped. Recurrent tumours with damaged envelopes show irregular-shaped lesions with ill-circumscribed margins.

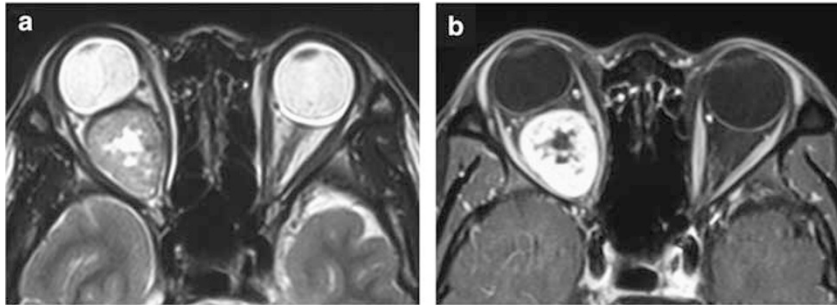


Figure 4 (a) Axial T2-weighted image showing an intraconal, cone-shaped mass extending from the retrobulbar to the orbital apex. The major portion is isointense, with a small patch of hyperintensity. (b) Axial gadolinium-enhanced T1-weighted image showing hyperintensity in the major portion of the mass, with a small patch of hypointensity.

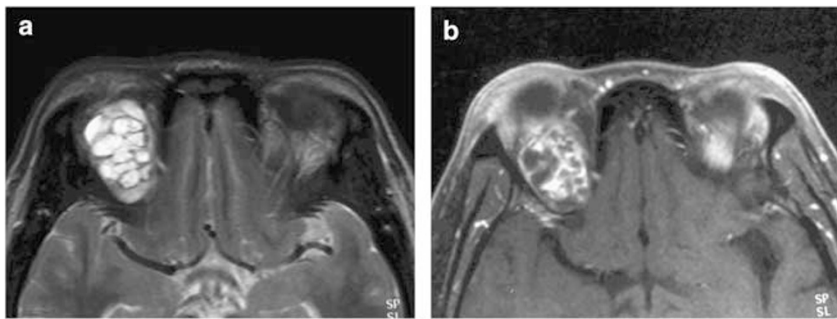


Figure 5 (a) Axial T2-weighted image showing a mass in the superior aspect of the right orbit. The major portion is hyperintense, with small, hypointense, strip-shaped areas. (b) Axial gadolinium-enhanced T1-weighted image showing hypointensity in the major portion of the mass, with small, hyperintense strip-shaped areas.

In our study, almost one-half of the tumours were located in the superior or medial superior aspect of the orbit. This correlates with the observation that orbital schwannomas most commonly arise from the supratrochlear or supraorbital branch of the trigeminal nerve.⁷

Previous studies have described orbital schwannomas as showing a low signal on T1-weighted and a high signal on T2-weighted images.^{6,8-11} On enhanced T1-weighted images, the lesions show homogeneous⁹⁻¹¹ or heterogeneous³ enhancement. Our data in this series of 62 cases demonstrate that there are additional characteristics, which may be of value in the clinical investigation of schwannomas. We know from our own experience, and that of other authors,^{5,12,13} that the histology of these lesions underlies the variation in their appearance on MRI. Microscopically, two distinct cellular patterns are seen, designated Antoni A and Antoni B. Antoni-A tissue is rich in cells and is composed of compact bundles of fibrillated cells. Antoni-B tissue is hypocellular and is composed of a loosely textured stroma. Both types of tissue often coexist in the same tumour and the latter does not necessarily predominate.¹⁴ Heterogeneity in MRI signal intensity is

due to the diversity of morphology, which may include intratumoural cysts, areas of different cellular patterns, calcifications, and regions of haemorrhage.¹⁵ Moreover, pathological characteristics frequently vary across different regions of the same tumour. In our series, surgical removal was usually carried out intracapsularly in a piecemeal fashion, thus producing tumour samples in the form of small pieces. This makes it much more difficult to delineate the relationship between local pathological characteristics and the signal observed on MRI. Our intention was to address this problem by describing our MRI findings on orbital schwannomas and proposing a possible association.

In our series, on unenhanced T1-weighted images, over one-half of the lesions demonstrated uniform isointensity; the remainder showed isointensity with patches or centres of hypointensity. These features are relatively nonspecific and correspond with the observations of other authors.^{5,9,10,12,13} It is our opinion that, compared with enhanced T1- and T2-weighted images, unenhanced T1-weighted images have less value in the differential diagnosis of schwannoma. Some of the features of schwannoma, including a well-circumscribed round or ovoid shape, iso- or hypointensity on

T1-weighted imaging, solitary fibrous tumours,¹⁶ isolated neurofibromas,¹⁷ cavernous hemangiomas,¹⁸ and meningiomas, are shared by a number of other orbital lesions.¹⁹ It is difficult to distinguish these lesions from those of schwannoma on T1-weighted images.

The use of gadopentetate dimeglumine as contrast material improves the sensitivity of MRI by selectively increasing the level of contrast enhancement in all schwannomas.²⁰ In our study, enhancement of T1-weighted images revealed five patterns of features. Importantly, some of these features correlate with the signal characteristics seen on T2-weighted images. The most common, occurring in over one-quarter of cases, was peripheral (ring) enhancement. On T2-weighted images, the central areas of lesions showed hyperintensity with peritumoural iso- or hypointensity. Correspondingly, on enhanced T1-weighted images, the central areas decreased to hypointensity and the peripheries increased to hyperintensity. Although cases of orbital cystic schwannoma with an enhancing capsule and a hypointense centre have been reported,^{4,5,1} this type of schwannoma is considered to be very rare. Schwannomas with one or several small cysts are likely to be more common than cystic schwannomas. Both types show peripheral enhancement on MRI and schwannomas with several cysts may show several enhanced rings. Cysts have been detected on MRI in 20% of vestibular schwannomas.²¹ Peripheral enhancement also corresponds with increases in cellular Antoni-A regions centrally and myxoid Antoni B regions peripherally.²² Moreover, it has been reported that hyaline thickening of vessel walls, cyst formation, and myxoid change in Antoni-B tissue occur frequently in peripherally enhanced lesions.¹³ Other authors have argued that peripheral enhancement is not necessarily synonymous with cyst formation and necrosis; it might also reflect poor central vascularity and/or increased compactness of the tumour, with decreased extracellular space available for contrast accumulation.²³

Our series of patients included two cases of peripheral (ring) non-enhancement that were well-enhanced centrally on enhanced T1-weighted images. This sign is very rare, in our experience. The principle outlined above, with interchanged locations, may provide an explanation.

On T2-weighted images, the Antoni-A regions show iso- or hypointensity and can be enhanced by the administration of contrast material.⁹ The finding that 16 tumours with homogeneous iso- or hypointensity on T2-weighted images showed homogeneous enhancement on T1-weighted images can thus be explained. Relatively abundant Antoni-A regions may be present in these tumours. However, both Antoni-A and Antoni-B tissue often coexist in the same tumour. Focal areas of

hyperintensity on T2-weighted images frequently correspond with cystic portions originating in Antoni B tissue, whereas hypointensity may represent haemorrhage, dense cellularity, collagen deposition,²⁴ calcification, or hyalinized stroma²⁵ that are not enhanced on enhanced T1-weighted images. Conversely, Antoni-A tissue and myxoid portions are well enhanced. Consequently, in our series, on T2-weighted images, 17 lesions were iso- to hypointense in the major portion with small patches of hyperintensity. Nine lesions were hyperintense in the major portion, with small patches of hypointensity. These 26 lesions showed mixed hypo- and hyperintensity on enhanced T1-weighted images. This pattern of heterogeneous enhancement, indicating histological diversity, may reflect a transitional state between peripheral and homogeneous enhancement. For example, as fusion and extension of small cystic portions occurs, small patches of non-enhanced areas become one large, non-enhanced central area with peripheral enhancement. Similarly, with an increase in Antoni-A regions, small patches of enhanced areas show homogeneous enhancement in a whole lesion. Calcification, collagen deposition, and other histological features contribute to the appearance of hypointensity on T2-weighted images and the absence of enhancement on enhanced T1-weighted images.

Preoperative diagnosis of orbital schwannoma is difficult. Our study has demonstrated features observable on MRI, which, when seen together with the target sign, peripheral enhancement, suggest the diagnosis of orbital schwannoma.

References

- 1 Tokugawa J, Nakao Y, Mori K, Maeda M. Orbital cystic neurinoma. *Acta Neurochir* 2003; **145**: 605–606.
- 2 Subramanian N, Rambhatia S, Mahesh L, Menon SV, Krishnakumar S, Biswas J *et al*. Cystic schwannoma of the orbit – a case series. *Orbit* 2005; **24**: 125–129.
- 3 Kanemoto Y, Okamoto S. Neurinoma of the short ciliary nerve: a case report. *No Shinkei Geka* 1994; **22**: 573–576.
- 4 Lam DS, Ng JS, To KF, Abdulah V, Liew CT, Tso MO. Cystic schwannoma of the orbit. *Eye* 1997; **11**: 798–800.
- 5 Abe T, Kawamura N, Homma H. MRI of orbital schwannomas. *Neuroradiology* 2000; **42**: 466–468.
- 6 Gunduz K, Shields CL, Gunalp I, Erden E, Shields JA. Orbital schwannoma: correlation of magnetic resonance imaging and pathologic findings. *Graefes Arch Clin Exp Ophthalmol* 2003; **241**: 593–597.
- 7 Jakobiec FA, Font RL. Peripheral nerve sheath tumours. In: Spencer WH (ed). *Ophthalmic Pathology*. Saunders: Philadelphia, PA, 1986, pp 2616–2626.
- 8 Bergin DJ, Parmley V. Orbital neurilemmoma. *Arch Ophthalmol* 1988; **106**: 414–415.
- 9 Shen WC, Yang DY, Ho WL, Ho YJ, Lee SK. Neurilemmoma of the oculomotor nerve presenting as an orbital mass: MR findings. *Am J Neuroradiol* 1993; **14**: 1253–1254.

- 10 Carroll GS, Haik BG, Fleming JC, Weiss RA, Mafee MF. Peripheral nerve tumours of the orbit. *Radiol Clin North Am* 1999; **37**: 195–202.
- 11 Torossian JM, Beziat JL, Abou Chebel N, Devouassoux-S M, Fischer G. Extracranial cephalic schwannomas. A report based on a series of 13 patients. *Ann Chir Plast Esthet* 1998; **43**: 541–547.
- 12 Mulkens TH, Panize PM, Martin JJ, Degryse HR, Van HP, Forton GE *et al.* Acoustic schwannoma: MR findings in 84 tumours. *Am J Radiol* 1993; **160**: 395–398.
- 13 David PF, Lisa MT, Adam EF. Intradural schwannomas of the spine: MR findings with emphasis on contrast-enhancement characteristics. *Am J Radiol* 1992; **158**: 1347–1350.
- 14 Russell DS, Rubinstein LJ. *Pathology of Tumours of the Nervous System*, 5th edn. Williams & Wilkins: Baltimore, 1989.
- 15 Goldberg HI. Extraaxial brain tumours. In: Atlas, SW (ed). *Magnetic Resonance Imaging of the Brain and Spine*. Raven Press: New York, 1991, pp 327–377.
- 16 DeBacker CM, Bodker F, Putterman AM, Beckmann E. Solitary fibrous tumour of the orbit. *Am J Ophthalmol* 1996; **121**: 447–449.
- 17 Park WC, White WA, Woog JJ, Garrity JA, Kim YD, Lane J *et al.* The role of high-resolution computed tomography and magnetic resonance imaging in the evaluation of isolated orbital neurofibromas. *Am J Ophthalmol* 2006; **142**: 456–463.
- 18 Thorn-Kany M, Arrue P, Delisle MB, Lacroix F, Lagarrigue J, Manelfe C. Cavernous hemangioma of the orbit: MR imaging. *J Neuroradiol* 1999; **26**: 79–86.
- 19 Weber AL, Sabates NR. Survey of CT and MR imaging of the orbit. *Eur J Radiol* 1996; **22**: 42–52.
- 20 Breger AK, Papke RA, Potunas KW, Haughton VM, Williams AL, Daniels DL. Benign extraaxial tumours: contrast enhancement with Gd-DTPA. *Radiology* 1987; **163**: 427–429.
- 21 Tali E, Yuh W, Nguyen H, Feng G, Koci TM, Jinkins JR *et al.* Cystic acoustic schwannomas: MR characteristics. *Am J Neuroradiol* 1993; **14**: 124–127.
- 22 Murphey MD, Smith WS, Smith SE, Kransdorf MJ, Temple HT. From the archives of the AFIP: imaging of musculoskeletal neurogenic tumours – radiologic-pathologic correlation. *RadioGraphics* 1999; **19**: 1253–1280.
- 23 Sze G, Bravo S, Krol G. Spinal lesions: quantitative and qualitative temporal evolution of gadopentetate dimeglumine enhancement in MR imaging. *Radiology* 1989; **170**: 849–856.
- 24 Demachi H, Takashima T, Kadoya M, Suzuki M, Konishi H, Tomita K *et al.* MR imaging of spinal neurinomas with pathological correlation. *J Comput Assist Tomogr* 1990; **14**: 250–254.
- 25 Zagardo MT, Castellani RJ, Rees JH, Rothman MI, Zoarski GH. Radiologic and pathologic findings of intracerebral schwannoma. *Am J Neuroradiol* 1998; **19**: 1290–1293.